

Sirt3 Regulates Radioresistance of Non-small Cell Lung Cancer through ATM-Chk2 Pathway

Cao Kun (✉ seeu_tomorrow@163.com)

second military medical university <https://orcid.org/0000-0001-9031-2646>

Chen Yuanyuan

second military medical university

Huang Yijuan

second military medical university

Liao Zebin

second military medical university

Liu Tingting

second military medical university

Gong Zhenyu

second military medical university

Cai Jianming

second military medical university

Cui Jianguo

second military medical university

Yang Yanyong

second military medical university

Gao Fu

second military medical university

Research

Keywords: Sirt3, Radiosensitivity, Lung cancer, DNA damage

Posted Date: April 8th, 2020

DOI: <https://doi.org/10.21203/rs.3.rs-20854/v1>

License: © ⓘ This work is licensed under a Creative Commons Attribution 4.0 International License.

[Read Full License](#)

Abstract

With high incidence and mortality, non-small cell lung cancer (NSCLC) represent 85-90% in all lung cancer patients. In addition to surgery and chemotherapy, radiotherapy is an indispensable approach for cancer treatment. However, cellular resistance to ionizing radiation often results in failure in treatment. In this study, we aimed to investigate the role of Sirt3 in radiotherapy on NSCLC. Briefly, survival as well as apoptosis assay were used to determine the cellular radiosensitivity, and an in situ lung cancer model to test the radiosensitivity in vivo. Firstly, our data show that Sirt3 is upregulated in NSCLC cell lines, as well as tissues compared with normal tissues. Then we generated Sirt3 knockdown cells and overexpression cells and found that Sirt3 knockdown increased radiosensitivity, while Sirt3 overexpression caused resistance. Sirt3 knockdown also aggravated the G2/M cell cycle arrest caused by irradiation. Furthermore, Sirt3 was found to be critical for the activation of ATM-Chk2 pathway upon irradiation. Finally, our in vivo model showed that targeting Sirt3 significantly sensitized lung cancer to radiotherapy. In conclusion, our findings identified a significant role of Sirt3 in radioresistance of NSCLC, which provides novel mechanism as well as target for radiotherapy.

Introduction

Non-small cell lung cancer (NSCLC) accounts for approximately 85-90% and remains one of the leading causes of mortality worldwide¹. Besides surgery, chemotherapy as well as targeted therapy, radiotherapy represents a main strategy when used alone or combined with other adjuvant treatment². However, the basic or gradually resistance of cancer cells to ionizing radiation often leads to failure of therapy^{3,4}. The main reason is that the underlying mechanism of radioresistance is unclear and novel radiosensitizing target is to be identified.

Sirtuin 3 (Sirt3) is a member of sirtuins family of NAD-dependent deacetylases which mainly involve in aging and cell fate determination⁵. Recently, it has been shown that Sirt3 play critical roles in cancer progression as well as chemoresistance^{6,7}. Similar to Sirt6 and Sirt7, Sirt3 was also related to DNA damage repair signaling pathway, which is one of core mechanism of cancer radioresistance⁸. Previous study showed that Sirt3 is related to the malignancy of NSCLC^{9,10}. However, whether Sirt3 plays a role of oncogene or tumor suppressor in different cancer is still controversial. Moreover, there is no evidence whether sirt3 participate in radiation response of NSCLC.

In the present study, we checked the expression of Sirt3 in NSCLC cells and tissues. Sirt3 knockdown cells and overexpression cells was generated to study its influence on radiosensitivity and the downstream signaling pathways. Furthermore, by using our in situ lung cancer implantation model, we found that Sirt3 deficiency causes increased sensitivity of cancer cells to radiotherapy. Our data provide novel mechanism and target for NSCLC radiotherapy.

Results

Sirt3 is upregulated in NSCLC and responsive to ionizing radiation

Firstly, we examined the basal expression level of Sirt3 in human bronchial epithelial cells (BEAS-2B) and various human lung cancer cells (A549, H460, H1299) by Western Blotting assay. The results showed that the expression level of Sirt3 in lung cancer cells was much higher than in normal bronchial epithelial cells (Fig. 1A). We performed a tissues microarray by using patients samples and found that the expression level of Sirt3 in lung cancer tissues was considerably higher than that in paracancerous tissues (Fig. 1B). The TCGA database showed the same trend, in lung adenocarcinoma and lung squamous cell carcinoma, the expression level of Sirt3 in primary tumor was significantly higher than that in normal lung tissue adjacent to cancer. (Fig. 1C) Next, we explored whether irradiation has an impact on Sirt3 expression in human bronchial epithelial cell and lung cancer cells. The results showed that after 8Gy irradiation, the expression level of Sirt3 in BEAS-2B cell increased markedly at 8 hours after irradiation, while in lung cancer cells A549 and H1299, the Sirt3 expression level was significantly decreased at 12 hours after irradiation. (Fig. 1D)

Sirt3 affects the irradiation sensitivity and radiation-induced apoptosis in lung cancer cells

To investigate the effect of Sirt3 on the radiation sensitivity of lung cancer cells, we constructed Sirt3 knockdown shRNAs and overexpression plasmid, and further applied it to A549 cell by lentivirus infection, then verified their knockdown and overexpression efficiency by Western Blot (Fig. 2A). Next, we examined the irradiation effect on the cell viability of these cell lines by CCK-8, and found that Sirt3 knockdown cell was more sensitive to irradiation and show lower cell viability after irradiation (Fig. 2B). At the same time, we calculated the numbers of cell colonies on each group, explored A549 cell survival after irradiation by colony formation assay. It was found that Sirt3 knockdown cell formed fewer colonies after irradiation than NC group, further indicated that it is more sensitive to irradiation, while Sirt3 overexpression cell was not significantly different from the NC group (Fig. 2C). By using flow cytometry assay, we found that after 8Gy irradiation, the proportion of apoptotic cells in Sirt3 knockdown group was significantly higher than that in NC group, while the percentage of apoptotic cells in Sirt3 overexpression group was significantly decreased (Fig. 2D).

Sirt3 promote radiation-induced cell cycle arrest and DNA damage repair

Cells are largely arrested in the G2/M phase to repair the DNA damage caused by irradiation. Besides, irradiation can cause γ -H2AX foci, its enrichment can be used as a marker for DNA double-strand break damage. In this study, we found that in NC group, 8Gy irradiation caused serious G2/M cycle arrest of A549, and it was most severe in 12 hours after irradiation, then gradually recovered. In the Sirt3 knockdown group, the G2/M phase arrest caused by irradiation was more severe and the recovery was slower, indicated that the A549 cells in this group had more profound DNA damage and less repair efficiency. In contrast, the G2/M phase arrest in Sirt3 overexpression group was lighter and recovered faster than NC group (Fig. 3A). Sirt3 knockdown group showed a larger amount of γ -H2AX foci enrichment than NC group, and more foci were present until 8-12 hours after irradiation, indicated that

A549 cell with Sirt3 knockdown had more severe DSBs and slower DSBs repair after 4Gy irradiation. While results in the Sirt3 overexpression group were reversed. (Fig. 3B)

Sirt3 is required for the activation of ATM-Chk2 mediated DNA repair

To explore the role Sirt3 in DNA damage repair (DDR), proteins of each group at 0, 0.5, 6, and 12 hours were extracted after 8Gy irradiation. The results showed that in NC group, activation of ATR-Chk1 and ATM-Chk2 pathway occurred after irradiation, and the activation gradually diminished up to 24h. The phosphorylation of ATR and Chk1 in the Sirt3 knockdown group was consistent with NC group, while the activation of p-ATM and p-Chk2 at 0.5 hour was significantly inhibited. As an indicator of DNA damage, γ -H2AX level remains upregulated at later time points, which was consistent with the immunofluorescence results (Fig. 4).

Sirt3 confers radioresistance in in situ murine lung cancer model

In order to verify the in vivo effect of Sirt3 on lung cancer, we constructed a mouse lung cancer radiotherapy model, and implanted Sirt3 NC, knockdown, and overexpression Lewis lung cancer (LLC) cells in the left lower lung lobe of C57 mice. One week later, the mice were subjected to single localized γ -irradiation at a dose of 15 Gy on lung area. Survival results showed that the survival time of the Sirt3 NC and overexpression groups was less than 20 days, while the knockdown group had the longest survival time till 24 days, showed a significant survival advantage (Fig. 5A). General view of lung tissues showed that compared with the NC group, the lung tumor in Sirt3 knockdown group grew slower, and had more profound hemorrhagic necrosis. (Fig. 5B) In HE staining, we found the same trend, indicated that Sirt3 knockdown tumor cell was more severely damaged by irradiation at the same dose. (Fig. 5C & 5D) TUNEL staining can better reflect the degree of radiation-induced apoptosis of tumor cells, and Ki67 staining reflects the proliferation ability of tumor cells. Next, we found that in the Sirt3 knockdown group, radiation-induced apoptosis of tumor cells was more extensive and severe, reflected its better radiation sensitivity. At the same time, the proliferation ability of tumor cells in Sirt3 knockdown group was significantly weaker than that in NC group and Sirt3 OE group, indicated that the inhibit ability of radiation in this group was much stronger. (Fig. 5E) By immunohistochemical staining of Sirt3, p-ATM, p-Chk2 and γ -H2AX in each group of tumor tissues, it was also found that the activation of γ -H2AX was more pronounced in Sirt3 knockdown group, and the radiation-induced activation of p-ATM was significantly attenuated. However, in p-Chk2 immunofluorescence staining, compared to normal lung tissues, we did not find p-Chk2 positive staining cells in tumor tissues. (Fig. 5F)

Discussion

To our knowledge, this is the first study demonstrating the role of Sirt3 in radiosensitivity of non-small cell lung cancer (NSCLC). In this study, we demonstrated that Sirt3 is highly expressed in NSCLC cell lines, tissues, as well as patients data derived from TCGA database. As a radiation responsive gene, Sirt3 also participate in the radiation resistance of lung cancer cells, and knockdown Sirt3 sensitized cells to radiation treatment. Our data also showed that Sirt3 deficiency results in more cells arrested in G2/M

phase. Sirt3 is also required for the activation of ATM-Chk2 pathway, instead of ATR. Finally, using our in situ lung cancer model, we found that Sirt3 confers the radioresistance of lung cancer in vivo.

Radiotherapy is an indispensable strategy for NSCLC when used alone or combined with chemotherapy as well as targeted therapy^{11,12}. When some patients benefit from this technique, a large proportion are characterized with a radioresistant property¹³⁻¹⁵. Even for those sensitive, radioresistance gradually occurs as radiotherapy applied¹⁶. So people tried to identify novel radiosensitizing target to improve the therapy of lung cancer. Sirtuins are a family of silent information regulator (Sirtuins) which was firstly identified in aging the cellular senescence^{17,18}. Among all, Sirt1, Sirt6 and Sirt7 was demonstrated to involve in DNA damage repair, the over-activation of which accounts mainly for radioresistance of cancer^{19,20}. In the present study, we demonstrated that Sirt3 was also critical for the activation of ATM-Chk2 signaling pathway. However, the activation of ATR remains unchanged. These data indicated that Sirt3 might regulates ATM mediated HR repair. Moreover, we also found that Sirt3 deficiency caused impairment in DNA damage repair in terms of γ -H2AX foci. These findings provide novel mechanism of radioresistance in NSCLC.

Recently, Sirt3 was found to be involved in cancer development and progression^{8,21}. And Sirt3 is also critical for mitochondrial function, DNA damage, cell metabolism as well as cell apoptosis^{5,22}. Up to now, Sirt3 has been studied in many cancer types, including esophageal cancer²³, oral cancer²⁴, colon cancer²⁵, breast cancer²⁶ *etc.* However, whether Sirt3 plays a role as oncogene or tumor suppressor is still controversial²⁷. For lung cancer, it has been reported that Sirt3 is related to the poor prognosis²⁸. However, the role of Sirt3 in radiotherapy of lung cancer is unclear. Cellular radiosensitivity is the key basis of tumor radiation response. Then we determined the cellular response of NSCLC to ionizing radiation when Sirt3 is overexpressed or downregulated. In our present study, we found that cells with Sirt3 knockdown was sensitive to ionizing radiation, while Sirt3 overexpression increased the radioresistance of NSCLC cells. Knockdown of Sirt3 also enhanced radiation-induced apoptosis and G2/M cell cycle arrest. These data suggested that Sirt3 is related to a radioresistant phenotype, which provide a potential target for radiosensitization.

In vivo tumor model is critical for the evaluation of tumor progression and therapy. For lung cancer radiotherapy, several animal models has been developed for the study of cancer response according to previous studies^{29,30}. For instance, subcutaneous tumor bearing model is widely used when for test of drugs or radiotherapy³¹. Another model is Kras-induced lung cancer, in which mice was generated with a Kras mutant³⁰. However, neither the subcutaneous model nor Kras mutant model can reflect the real environment in lung cancer. In our present study, we generated an in situ lung cancer model, and we injected the Sirt3 modified cells directly into the lung tissues. After then, radiotherapy was applied. It was found that Sirt3 deficiency increased the radiosensitivity in vivo, and targeting Sirt3 also reduced the activation of DNA damage signaling pathway. These findings provide evidence that Sirt3 is potential therapeutic target in terms of animal model. However, we did not find p-Chk2 positive staining cells in tumor tissues, this phenomenon may be due to a significant decrease of phosphorylation Chk2 in tumor

cells 10 days after irradiation, or the expression level of p-Chk2 is too low in LLC cells, the specific cause needs to be identified in further experiments.

In conclusion, we demonstrated that Sirt3 is upregulated in NSCLC tissues and cell lines. As a radiation responsive gene, Sirt3 confers radioresistance in NSCLC cell lines in terms of survival assay and apoptosis assay. DNA damage repair impairment and cell cycle arrest was also observed in Sirt3 knockdown cells upon irradiation. Our findings provide novel mechanism of radiation resistance and suggests Sirt3 as a potential target of radiosensitization in NSCLC.

Materials And Methods

Cell culture and lentiviral shRNA infection

Human bronchial epithelial cell line BEAS-2B, non-small cell lung cancer cell line A549, H460, H1299 and mouse lewis lung cancer cell line LLC purchased from American Type Culture Collection (ATCC, VA, USA). All human cell lines used in this study have been authenticated by STR profiling in the year of 2019. All experiments were performed with mycoplasma-free cells.

BEAS-2B and H1299 were maintained in RPMI 1640 medium with 10% fetal bovine serum (Gibco, Grand Island, NY, USA), A549, H460 and LLC were maintained in DMEM medium with 10% fetal bovine serum (Gibco, Grand Island, NY, USA) at 37°C in a 5% CO₂ humidified chamber.

In this study, we constructed human Sirt3 scrambled shRNA (TTCTCCGAACGTGTCACGT), three shRNAs (GTGGGTGCTTCAAGTGTGTT, GTGGGTGCTTGGGTGTTGTT, AGTGTGCTTCAAGTGTGTT), and overexpresses lentiviral plasmid (Gene sequence from NCBI database) lentiviruses (made from the vector GV248). Besides, we also constructed mouse Sirt3 scrambled shRNA (TTCTCCGAACGTGTCACGT), three shRNAs (CTTCAATGCTTCAAGTGTGTT, GTGGGTGCTTGATGTTGTT, AGTGTGCTTCAAGTGTGTTATG), and overexpresses lentiviral plasmid (Gene sequence from NCBI database) lentiviruses. All these lentiviruses were generated by BioLink (Shanghai, China). Sirt3 plasmid lentiviral vectors were used for knockdown and overexpression of Sirt3. Cells were seeded at 1×10^5 cells/well into six-well plates and infected with lentiviral particles using polybrene (10 mg/mL). After infection, virus-containing medium was replaced with normal medium, and then cells were selected with puromycin (2 mg/mL). After cell infection, the knockdown effect of the three shRNAs in human and mouse were tested by Western Blot, then we selected the viral plasmids of the best knockdown effect, human Sirt3 shRNA (GTGGGTGCTTCAAGTGTGTT) and mouse Sirt3 shRNA (CTTCAATGCTTCAAGTGTGTT), for next experiments.

Animals and tumor planting

The whole protocols were approved by the Ethics Committee of Second Military Medical University. Male C57BL/6 mice, 8 weeks old, obtained from the Experimental Animal Center of Chinese Academy of Sciences (Shanghai, China), were used for the animal experiment. Mice were fed in daily-changed

individual cages, at $25\pm 1^{\circ}\text{C}$ with food and water provided for free access. The mice were randomly divided into three groups: group 1, negative control; group 2, Sirt3 knockdown; group 3, Sirt3 overexpression.

The mouse was anesthetized with isoflurane gas (VETEASY, Shenzhen, China), then placed the right side of the mouse on the operation table. The skin and superficial soft tissue were cut at the midline of left rib, and the insulin injection needle was inserted into the second last rib gap, and the depth of the needle was 2 mm, then the LLC cell was injected into the left lower lobe of the mouse at 1×10^6 per 25 μl . After skin sutured and disinfected, the mouse was resuscitated.

Irradiation

The ^{60}Co γ -rays in Radiation Center (Faculty of Naval Medicine, Second Military Medical University, Shanghai, China) were applied for the irradiation exposure. Cells were irradiated with 2, 4, 8 Gy at a dose rate of 1 Gy/min. After anesthetization with 10% chloral hydrate (350mg/kg), mice were subjected to whole-lung irradiation with 15Gy at a dose rate of 1Gy/min.

Western Blot

Cells were homogenized in mammalian protein extraction reagent (M-PER) to prepare a protein sample. The lysates were mixed with 10% SDS-PAGE then electrophoresis was performed on the same amount based on the concentration. After the electrophoresis, the protein was transferred to a nitrocellulose membrane (Amersham, Arlington Heights, IL, USA) then blocked with 5% milk for 1 hr at room temperature. The proteins were incubated with Sirt3 (1:1000), p-ATM (1:1000), p-ATR (1:1000), p-Chk1 (1:1000), p-Chk2 (1:1000), γ -H2AX (1:1000) and β -tubulin (1:1000) (Cell Signal Tech, Danvers, MA, USA) at 4°C overnight in a shaker incubator. After washing with TBS-T, the membranes were incubated with anti-rabbit or anti-mouse IgG horseradish peroxidase conjugated antibody (1:5000; Cell Signal Tech.) for 1 hr at room temperature. The protein bands were visualized using enhanced chemiluminescence with a Super Signal west pico kit (Bridgen Biological Technology, Shanghai, China). Films were scanned and analyzed by densitometry using Syngene GeneGenius software (Syngene, Frederick, MD, USA).

Cell viability assay

Cell viability was determined by Cell Counting Kit-8 (Dojindo, Kumamoto, Japan). Cells were suspended and seeded into 96-well plates with 5×10^3 cells/well. At the 48h after irradiation, cell viability was tested with a CCK-8 assay.

Clonogenic assay

Cells were trypsinized, counted, and seeded in 60-mm culture dishes for each dose of radiation. Sufficient numbers were seeded to ensure that approximately 30-100 macroscopic colonies would appear in each plate after 10-14 days. Colonies were stained with 0.5% gentian violet in methanol and counted. The plating efficiency (PE) for each dose was calculated by dividing the number of colonies by the number of

cells plated and expressing the result as a percentage. The surviving fraction was calculated by dividing the PE of the irradiation groups by the PE of the appropriate unirradiated control.

Apoptosis analysis

Apoptosis of cells with or without irradiation was determined by Annexin V-PE and 7-AAD staining. The cells were plated in six-well plates at a density of 10^5 cells per well and allowed to attach for 24h. The cells were harvested by trypsin digestion, washed with PBS twice, and resuspended 24h after irradiation. Then the cells were stained with Annexin V-PE and 7-AAD at room temperature for 15 min in a dark room according to the Annexin V-PE/7-AAD Apoptosis Detection Kit (YEASEN, Shanghai, China) instructions.

Cell cycle analysis

Cell cycle was analyzed by PI staining. The cells were plated in six-well plates at a density of 2×10^6 cells per well and allowed to attach for 24h. The cells were harvested by trypsin digestion in 0, 8, 12, 24h after irradiation, then washed with PBS twice, fixed with pre-cooled 75% ethanol for 24 h, then washed again twice with PBS, and stained with PI for 30 min at 4 °C, and assayed by flow cytometer.

Histopathology

At indicated time points, lung tissues were isolated and subjected to sectioning, then the samples were stained with H&E, terminal transferase-mediated dUTP nick end labeling (TUNEL), Ki67 (1:400, Cell Signal Tech, Danvers, MA, USA), Sirt3 (1:200, Cell Signal Tech, Danvers, MA, USA), p-ATM (1:100, Cell Signal Tech, Danvers, MA, USA), p-Chk2 (1:200, Cell Signal Tech, Danvers, MA, USA), and γ -H2AX (1:200, Cell Signal Tech, Danvers, MA, USA) staining. Five fields per section at 200 magnifications were randomly selected per mouse, and two blinded pathologists independently examined 30 fields per group using Nikon DS-Fi1-U2 microscope (Nikon, Tokyo, Japan).

Immunofluorescence staining

Immunofluorescence analysis was performed to measure the expression of γ -H2AX in A549 cells. After fixed with 4% formaldehyde solution, the slides were incubated with γ -H2AX (1:200, Cell Signal Tech, Danvers, MA, US) antibodies at 4°C overnight. After washed with PBS, slides were incubated with Texas Red-conjugated anti-rabbit secondary antibodies (Cell Signal Tech, Danvers, MA, US) at room temperature for 30 min. Nuclei were counterstained with DAPI, and the slides were analyzed by using a fluorescence microscope (Nikon Eclipse Ti-SR, Nikon, Tokyo, Japan).

Statistical analysis

Data was expressed as the means \pm standard error of the mean (SEM). Comparison between-group were performed using one-way ANOVA. Two-group comparisons were performed using independent-samples Student's *t*-test. $P < 0.05$ was considered significant. All experiments were performed at least 3 independent times.

Abbreviations

NSCLC, non-small cell lung cancer;

Sirt3, Sirtuin 3;

TCGA, the cancer genome atlas;

DSBs, double strand breaks;

DDR, DNA damage repair;

LLC, Lewis lung cancer.

Declarations

Ethical Approval and Consent to participate

Ethical approval was obtained from the Ethics Committee of Second Military Medical University. All the participants have written consent for this study

Data availability statement

The sequence of sirt3 overexpression plasmid that support the findings of this study are openly available in GeneCards at <https://www.genecards.org/cgi-bin/carddisp.pl?gene=SIRT3>.

Competing of interests

The authors declare that they have no competing interests.

Funding and Acknowledgment

This study was supported in part by grants from National Natural Science Foundation of China (No. 31670861, No. 11635014, No. 31700739, No. 81972968) and Shanghai association for science and technology (No. 20184Y0167).

Author's contributions

CK, CY, and HY carried out the design of the study and wrote the manuscript. LZ worked on the collection and analysis of the data. LT and GZ contributed to the conception of the study and the final approval of the final version of the manuscript submitted. CJ, YY, and GF contributed to the manuscript writing. CJ contributed to data interpretation and manuscript writing. All authors read and approved the final manuscript.

References

1. Molina JR, Yang P, Cassivi SD, Schild SE, Adjei AA. Non-small cell lung cancer: epidemiology, risk factors, treatment, and survivorship. *Mayo Clin Proc.* 2008;83(5):584-594.
2. McDonald F, Senan S, Faivre-Finn C, Hatton M. Curative Radiotherapy for Non-small Cell Lung Cancer: Practice Changing and Changing Practice? *Clin Oncol (R Coll Radiol).* 2019;31(10):678-680.
3. Zhu R, Yang X, Xue X, et al. Neuroendocrine differentiation contributes to radioresistance development and metastatic potential increase in non-small cell lung cancer. *Biochim Biophys Acta Mol Cell Res.* 2018;1865(12):1878-1890.
4. Klein C, Dokic I, Mairani A, et al. Overcoming hypoxia-induced tumor radioresistance in non-small cell lung cancer by targeting DNA-dependent protein kinase in combination with carbon ion irradiation. *Radiat Oncol.* 2017;12(1):208.
5. Chen Y, Fu LL, Wen X, et al. Sirtuin-3 (SIRT3), a therapeutic target with oncogenic and tumor-suppressive function in cancer. *Cell Death Dis.* 2014;5:e1047.
6. McDonnell E, Peterson BS, Bomze HM, Hirschev MD. SIRT3 regulates progression and development of diseases of aging. *Trends Endocrinol Metab.* 2015;26(9):486-492.
7. Bhat TA, Kumar S, Chaudhary AK, Yadav N, Chandra D. Restoration of mitochondria function as a target for cancer therapy. *Drug Discov Today.* 2015;20(5):635-643.
8. Pillai VB, Bindu S, Sharp W, et al. Sirt3 protects mitochondrial DNA damage and blocks the development of doxorubicin-induced cardiomyopathy in mice. *Am J Physiol Heart Circ Physiol.* 2016;310(8):H962-972.
9. Y X, M W, J Z, et al. SIRT3 is correlated with the malignancy of non-small cell lung cancer. *International journal of oncology.* 2017;50(3):903-910.
10. GC Y, BC F, DY Z, et al. The Expression and Related Clinical Significance of SIRT3 in Non-Small-Cell Lung Cancer. *Disease markers.* 2017;2017(undefined):8241953.
11. Wang C-M, Gao Y-L, Yin L-X. Current status and progress of radiotherapy for non-small cell lung cancer. *Chinese Journal of Cancer Prevention & Treatment.* 2017;24(10):720-724.
12. Couñago F, Rodríguez A, Calvo P, et al. Targeted therapy combined with radiotherapy in non-small-cell lung cancer: a review of the Oncologic Group for the Study of Lung Cancer (Spanish Radiation Oncology Society). *Clinical & Translational Oncology.* 2017;19(1):31-43.
13. Sun C, Zeng X, Guo H, et al. MicroRNA-125a-5p modulates radioresistance in LTP-a-2 non-small cell lung cancer cells by targeting SIRT7. *Cancer Biomark.* 2019.
14. Jiang W, Jin G, Cai F, et al. Extracellular signal-regulated kinase 5 increases radioresistance of lung cancer cells by enhancing the DNA damage response. *Exp Mol Med.* 2019;51(2):19.
15. Gokyildirim MY, Grandel U, Hattar K, et al. Targeting CREB-binding protein overrides LPS induced radioresistance in non-small cell lung cancer cell lines. *Oncotarget.* 2018;9(48):28976-28988.
16. Chen X, Wang P, Guo F, et al. Autophagy enhanced the radioresistance of non-small cell lung cancer by regulating ROS level under hypoxia condition. *Int J Radiat Biol.* 2017;93(8):764-770.

17. de Oliveira MV, Andrade JM, Paraiso AF, Santos SH. Sirtuins and cancer: new insights and cell signaling. *Cancer Invest.* 2013;31(10):645-653.
18. McGuinness D, McGuinness DH, McCaul JA, Shiels PG. Sirtuins, bioageing, and cancer. *J Aging Res.* 2011;2011:235754.
19. Rizzo A, Iachettini S, Salvati E, et al. SIRT6 interacts with TRF2 and promotes its degradation in response to DNA damage. *Nucleic Acids Res.* 2017;45(4):1820-1834.
20. Tang M, Li Z, Zhang C, et al. SIRT7-mediated ATM deacetylation is essential for its deactivation and DNA damage repair. *Sci Adv.* 2019;5(3):eaav1118.
21. Jablonski RP, Kim SJ, Cheres P, et al. SIRT3 deficiency promotes lung fibrosis by augmenting alveolar epithelial cell mitochondrial DNA damage and apoptosis. *FASEB J.* 2017;31(6):2520-2532.
22. Chen J, Wang A, Chen Q. SirT3 and p53 Deacetylation in Aging and Cancer. *J Cell Physiol.* 2017;232(9):2308-2311.
23. Zhao Y, Yang H, Wang X, Zhang R, Wang C, Guo Z. Sirtuin-3 (SIRT3) expression is associated with overall survival in esophageal cancer. *Annals of Diagnostic Pathology.*17(6):483-485.
24. Sirtuin-3 (SIRT3), a novel potential therapeutic target for oral cancer.117(8):1670-1678.
25. Liu C, Huang Z, Jiang H, Shi F. The Sirtuin 3 Expression Profile Is Associated with Pathological and Clinical Outcomes in Colon Cancer Patients. *Biomed Research International.* 2014;2014(5795):871263.
26. Desouki MM, Doubinskaia I, Gius D, Abdulkadir SA. Decreased mitochondrial SIRT3 expression is a potential molecular biomarker associated with poor outcome in breast cancer. *Human Pathology.*45(5):1071-1077.
27. Alhazzazi TY, Kamarajan P, Verdin E, Kapila YL. SIRT3 and cancer: tumor promoter or suppressor? *Biochim Biophys Acta.* 2011;1816(1):80-88.
28. Yang GC, Fu BC, Zhang DY, et al. The Expression and Related Clinical Significance of SIRT3 in Non-Small-Cell Lung Cancer. *Dis Markers.* 2017;2017:8241953.
29. Latteyer S, Christoph S, Theurer S, et al. Thyroxine promotes lung cancer growth in an orthotopic mouse model. *Endocr Relat Cancer.* 2019.
30. Rakhit CP, Trigg RM, Le Quesne J, et al. Early detection of pre-malignant lesions in a KRAS(G12D)-driven mouse lung cancer model by monitoring circulating free DNA. *Dis Model Mech.* 2019;12(2).
31. Weibel S, Hofmann E, Basse-Luesebrink TC, et al. Treatment of malignant effusion by oncolytic virotherapy in an experimental subcutaneous xenograft model of lung cancer. *J Transl Med.* 2013;11:106.

Figures

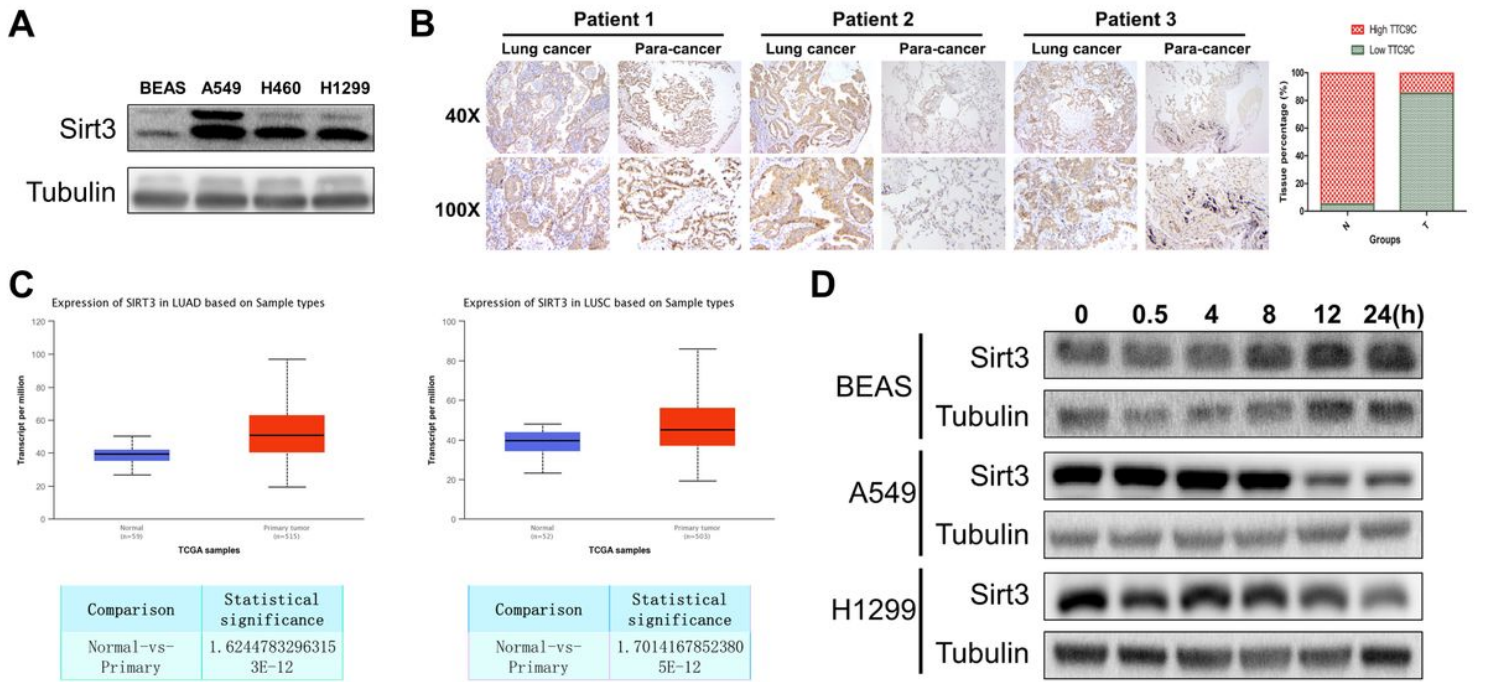


Figure 1

Sirt3 is highly expressed in cells and tissues of lung cancer, its expression is sensitive to irradiation. (A) Western Blot analysis of Sirt3 expression in bronchial epithelial cells and different lung cancer cells. (B) Representative images of Sirt3 tissue microarray of clinical lung cancer and their paracancerous tissue samples. (C) The expression of Sirt3 in lung adenocarcinoma (n=59 for normal tissue, n=515 for lung adenocarcinoma tissue, $p < 0.001$) and lung squamous cell carcinoma (n=52 for normal tissue, n=503 for lung squamous cell carcinoma tissue, $p < 0.001$). (D) Western Blot analysis of Sirt3 expression in bronchial epithelial cells and different lung cancers after 8Gy irradiation at different time points. Values are given as mean \pm SEM (n = 6 for each group per time point).

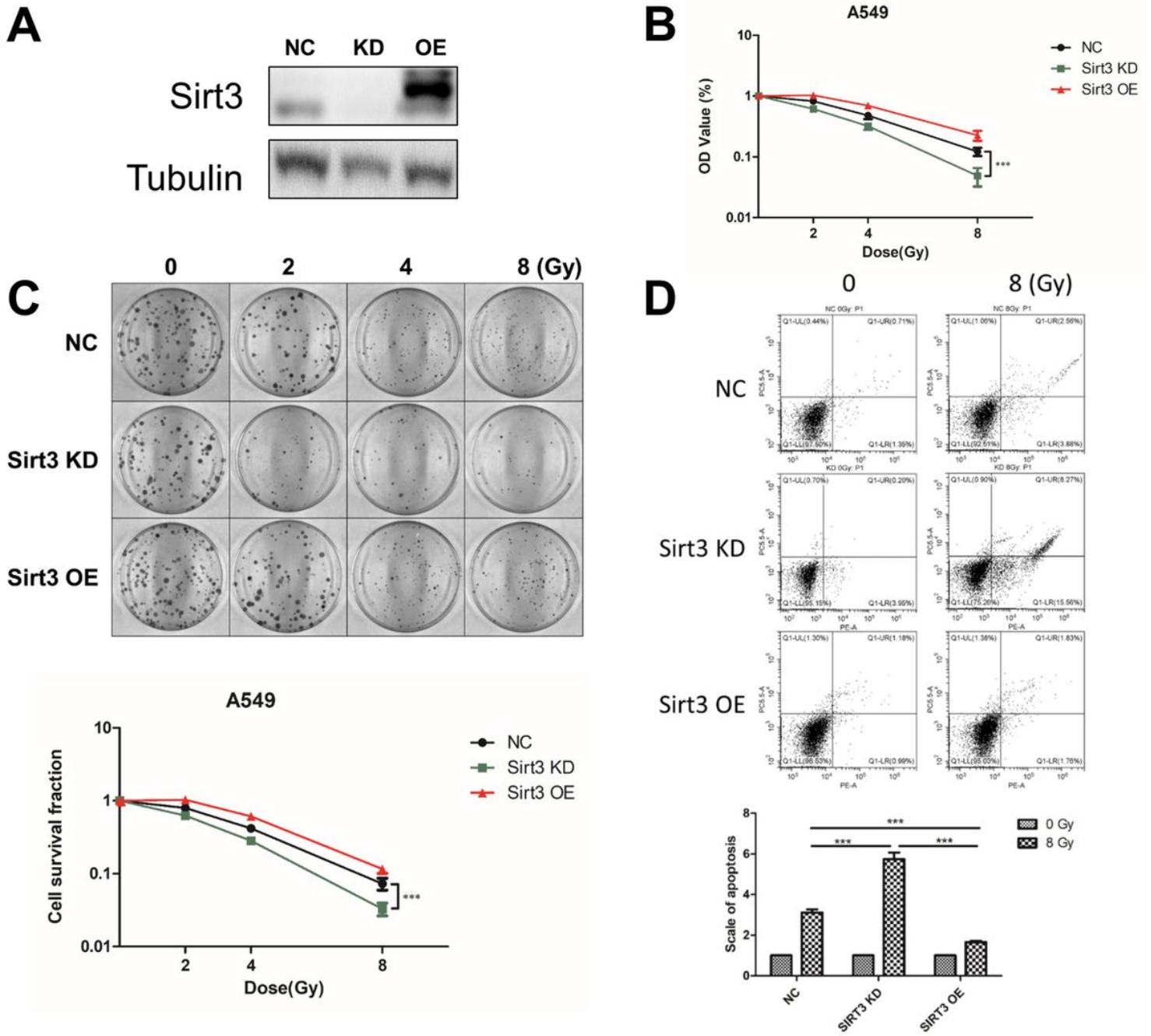


Figure 2

Sirt3 affects the irradiation sensitivity and radiation-induced apoptosis of lung cancer cells. (A) Representative western blot of Sirt3 following infection with Sirt3-specific shRNA and overexpression lentivirus. (B) A549 cell viability in different groups after 0, 2, 4, 8 Gy irradiation determined by CCK-8 assay. (C) A549 cell survival and its representative images in different groups after 0, 2, 4, 8 Gy irradiation was determined by colony formation. (D) The apoptosis of A549 after 8Gy irradiation at 24h in different groups was analyzed by flow cytometry. Values are given as mean±SEM (n = 6 for each group per time point), ***P<0.001 versus negative control shRNA group.

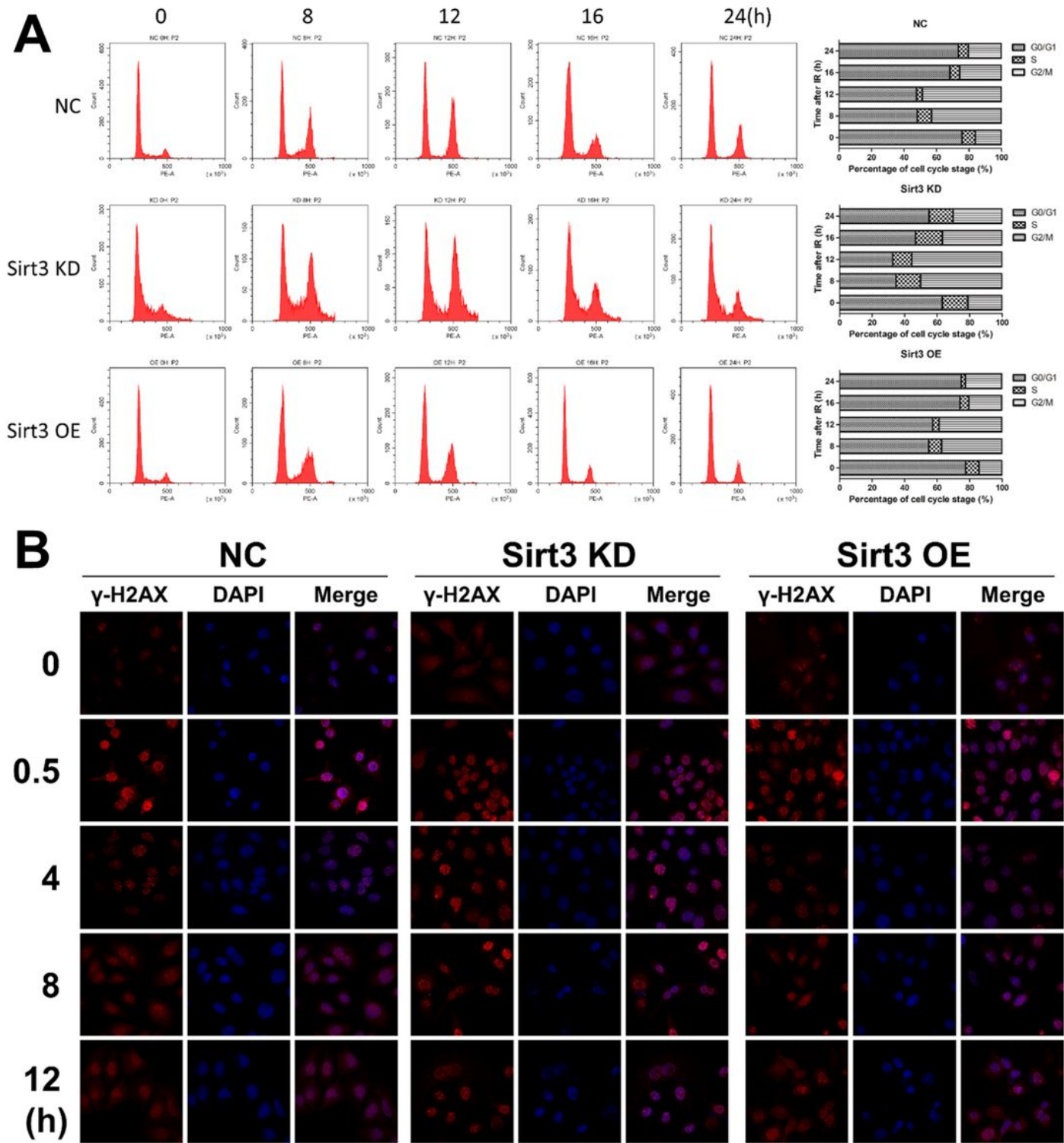


Figure 3

Sirt3 affects the process of radiation-induced cell cycle arrest and DNA damage repair. (A) The cell cycle of A549 after 8Gy irradiation in different groups was analyzed by flow cytometry. (B) The γ -H2AX foci in A549 after 4Gy irradiation in different groups was analyzed by immunofluorescence staining. Values are given as mean \pm SEM (n = 6 for each group per time point).

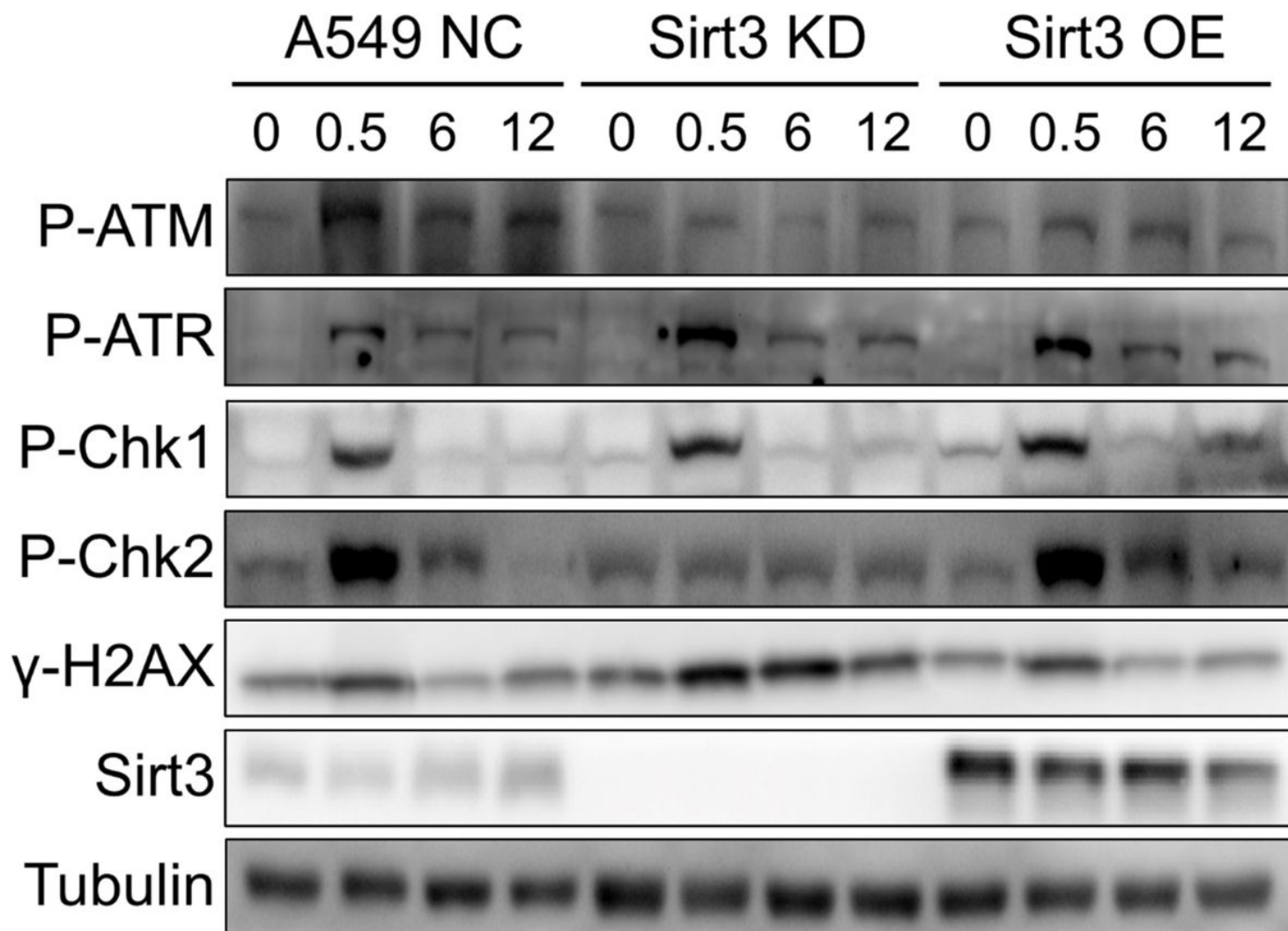


Figure 4

The function of Sirt3 relies on p-ATM-p-Chk2 pathway. Western Blot analysis of the protein expression in DNA Damage Response pathway in A549 after 8Gy irradiation at different time points.

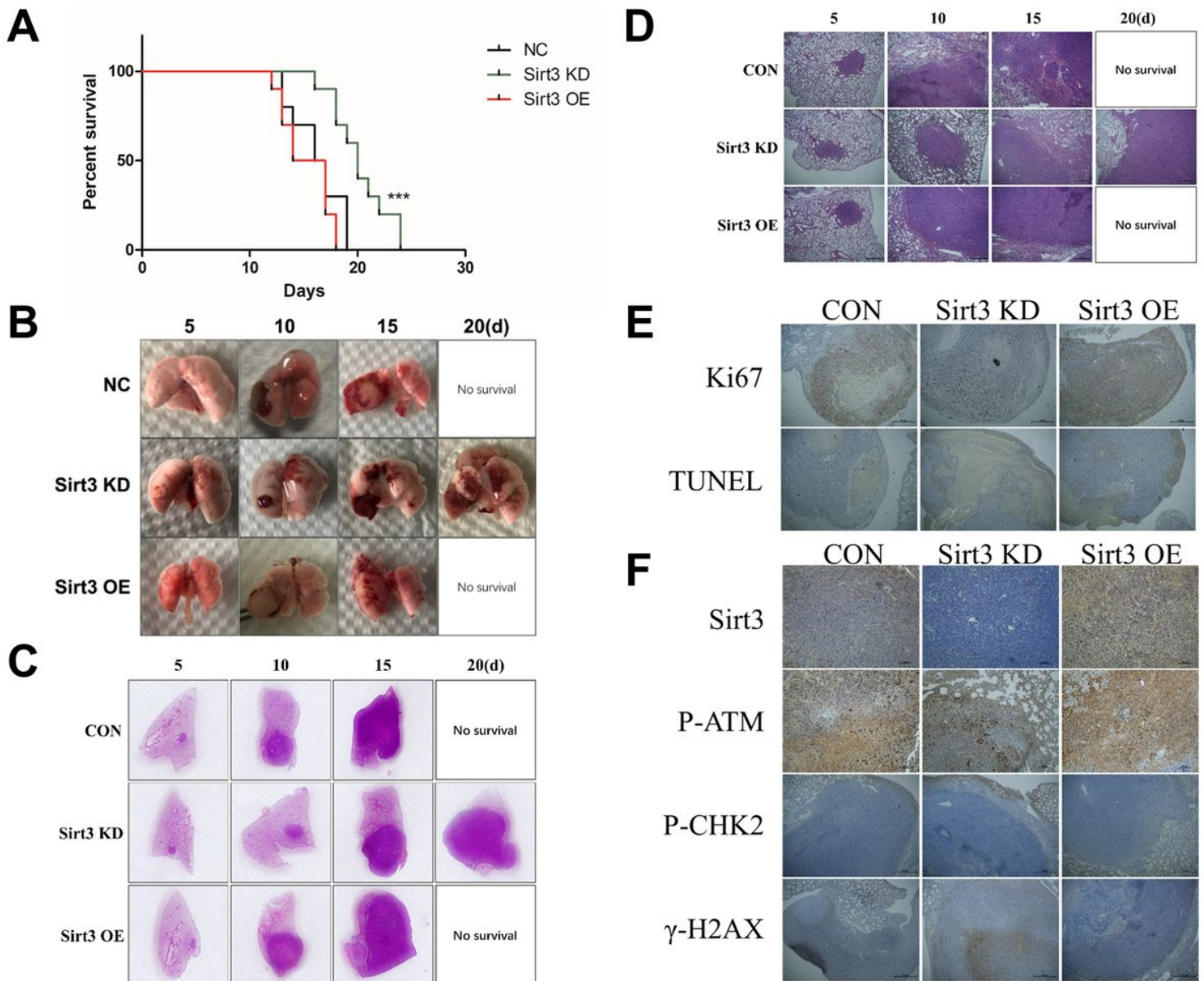


Figure 5

Sirt3 confers radioresistance in in situ murine lung cancer model. (A) The animal survival of lung tumor-bearing mouse model in different groups after 15Gy local irradiation in chest. (B) Representative images of lung tissue in different groups from 5 to 20 days after 15Gy local irradiation in chest. (C) and (D) Representative 1× and 40× images of HE immunohistochemical staining of lung tissue sections in different groups at 5 to 20 days after 15Gy local irradiation in chest. (E) Representative 40× images of Ki67 and TUNEL immunohistochemical staining of lung tissue sections in different groups at 10 days after 15Gy local irradiation in chest. (F) Representative 100× images of Sirt3, p-ATM, p-Chk2, and γ-H2AX immunohistochemical staining of lung tissue sections in different groups at 10 days after 15Gy local irradiation in chest. Values are given as mean±SEM (n = 6 for each group per time point), ***P<0.001 versus negative control shRNA group.